Applied Composite Materials **2:** 233–243, 1995.

Determining the Power Spectral Density of the Waviness of Unidirectional Glass Fibres in Polymer Composites

A. R. CLARKE, G. ARCHENHOLD and N. C. DAVIDSON
Department of Physics, University of Leeds, Leeds LS2 9JT, U.K.

W. S. SLAUGHTER
Department of Mechanical Engineering, University of Pittsburgh, 532 Benedum Hall, Pittsburgh, PA 15261, U.S.A.

and

N. A. FLECK
Department of Engineering, University of Cambridge, Trumpington Street, Cambridge, CB2 1PZ, U.K.

(Received 25 August 1995)

Abstract. A pilot study has been completed into the accurate measurement of 3D fibre waviness in high packing fraction, unidirectional, glass fibre reinforced polymer epoxy. It has been shown that the confocal laser scanning microscope (CLSM) can determine fibre waviness amplitudes, $A \leqslant 40$ μm and *simultaneously* fibre wavelengths, $\lambda \leqslant 4$ mm. Knowing the fibre-centre coordinates in 3D with sub-micron precision, the fibre waviness may be characterised in terms of the power spectral densities S_u and S_w orthogonal to the fibre direction (taken to be in the y direction) and also in terms of the power spectral densities of fibre slopes, $S_{u'}$ and $S_{w'}$. In future studies, these characterisation parameters will enable models linking random fibre waviness to compressive strength to be evaluated.

Key words: power spectral density, 3D fibre waviness, confocal laser scanning microscopy, high spatial resolution, characterisation, glass fibre reinforced, polymer composites.

1. Introduction

There has been considerable interest over the past few years [1–3] in the waviness of 'unidirectional' glass and carbon fibres in fibre-reinforced polymer composites and speculation of the effect of fibre waviness on a wide range of mechanical properties. A number of researchers have sought to measure both fibre and ply waviness [4–6] by 2D image analysis. However, the main optical technique for characterising fibre waviness has been to measure the fibre angular misalignments, Φ in a 2D section plane. If the fibre waviness is assumed to be

sinusoidal, the angular misalignments will be determined by the ratio of fibre waviness amplitude, A to wavelength, λ

$$\Phi \leqslant 2\pi A/\lambda \text{ radians} \tag{1}$$

Clearly this technique cannot determine both the fibre waviness amplitude and wavelength *simultaneously*.

In order to develop models linking fibre waviness to mechanical properties such as compressive strength, it has been assumed that fibre waviness is essentially a 2D phenomenon with typical values of 20 μm $< A <$ 50 μm for the wave amplitudes and 0.5 mm $< \lambda <$ 2 mm for the fibre wavelengths [7]. However, in reality, fibre waviness is a 3D phenomenon and hence there is a need for a measurement technique which shows submicron spatial resolution in x, y and z and which is capable of following fibres semi-automatically over significant distances (many mm). Data on 3D fibre-centre coordinates could, for example, indicate the extent to which neighbouring fibres show correlated movement; gross ply misalignments could also be distinguished from fibre waviness. It has been argued that the power spectral densities, S_u and S_w are useful measures of random fibre waviness for the prediction of compressive strength [8].

Take the nominal fibre direction to be aligned with the y-axis of a (x, y, z) Cartesian coordinate frame. The individual misalignment of each fibre is given by its deviation 'u' in the x-direction and its deviation 'w' in the z-direction from the mean path of the fibre. The deviation is measured at the centre of the fibre cross-section. In order to define the mean path for each fibre, straight lines are fitted to each fibre and subtracted out so that each fibre has zero mean deviation and zero mean slope.

For a fibre of infinite length, the autocorrelation function for waviness in the x-direction is defined as

$$\mathfrak{R}_u(\Delta) \equiv \int_{-\infty}^{\infty} u(y) \cdot u(y + \Delta)\, \mathrm{d}y. \tag{2}$$

The spectral density S_u is defined as the Fourier Transform of the autocorrelation function

$$S_u(\omega) = \frac{1}{2\pi} \int_{-\infty}^{\infty} \mathfrak{R}_u(\Delta) \cdot \mathrm{e}^{-i\omega\Delta}\, \mathrm{d}\Delta. \tag{3}$$

The spectral density curve is symmetric in ω and the area under $S_u(\omega)$ equals the mean square value E of $u(x)$

$$E[u^2] = \int_{-\infty}^{\infty} S_u(\omega)\, \mathrm{d}\omega. \tag{4}$$

If the fibre centre coordinates x, y and z are measured in μm, it follows that the dimensions of ω are [$\mu\mathrm{m}^{-1}$] and $S_x(\omega)$ are [$\mu\mathrm{m}^3$]. In practice, the fibres

are followed over a finite length, L and their centres are sampled every Δ μm. Therefore the Discrete Fourier Transform of $u(y)$ is required. If we write

$$u_k = u(y_k) \tag{5}$$

where $y_k = k\Delta$ (for $k = 0, 1, \ldots, N-1$) and $\Delta = L/N$, the Discrete Fourier Transform of u_k is

$$\aleph_k = \frac{1}{N} \sum_{r=0}^{N-1} u_r \, \mathrm{e}^{-i2\pi kr/N}. \tag{6}$$

To avoid aliasing, it is necessary to take $N > \omega_0 L/\pi$ where ω_0 is the maximum frequency component present in $u(y)$. It can be shown [9] that in discrete form, with

$$S_k = S_u(\omega_k) \tag{7}$$

and $\omega_k = 2\pi k/N\Delta$ (where $k = 0, 1, \ldots, N/2$), the spectral density is approximately given by

$$S_k = \frac{N\Delta}{2\pi} |\aleph_k|^2. \tag{8}$$

Therefore, if the loci of fibre centres were measured every 50 μm, the maximum frequency covered would be $\omega_{N-1} = \pi/\Delta = 6.28 \times 10^{-2}$ $\mu\mathrm{m}^{-1}$ which corresponds to the smallest measurable wavelength, $\lambda_{\min} = 100$ μm (because $\lambda = 2\pi/\omega$). Hence, the spectral density function, S_u indicates those wavelengths which dominate the fibre dataset. It has only recently been possible to acquire the sub-micron spatial resolution, fibre-centre coordinates over sample volumes of 200 μm $\times$ 5 mm $\times$ 40 μm within reasonable timescales.

2. Experimental

Confocal laser-scanning microscopy (CLSM) is capable of high spatial resolution, 3D measurements of glass-fibre reinforced polymer composites [10]. Unlike conventional optical reflection microscopy, optical sections can be thrown not only onto the sample surface, but also below the sample surface to a maximum depth determined by fibre-packing fraction and fibre opacity. Studies [11] have revealed that glass fibres are best detected when the CLSM is operated in fluorescence mode because most epoxy matrices fluoresce strongly when excited by the 488 nm argon-ion laser line. Polymer matrices which do not fluoresce at $\lambda > 488$ nm (e.g. polyoxymethylene, POM) may also be investigated because the sizing agents which coat the glass fibres usually fluoresce strongly and hence indicate the location of the fibres. The measurements described below were made using a Biorad Microscience MRC500 confocal laser scanning microscope system with a Nikon oil objective lens (NA 1.4, $\times$60). The spatial resolution of this

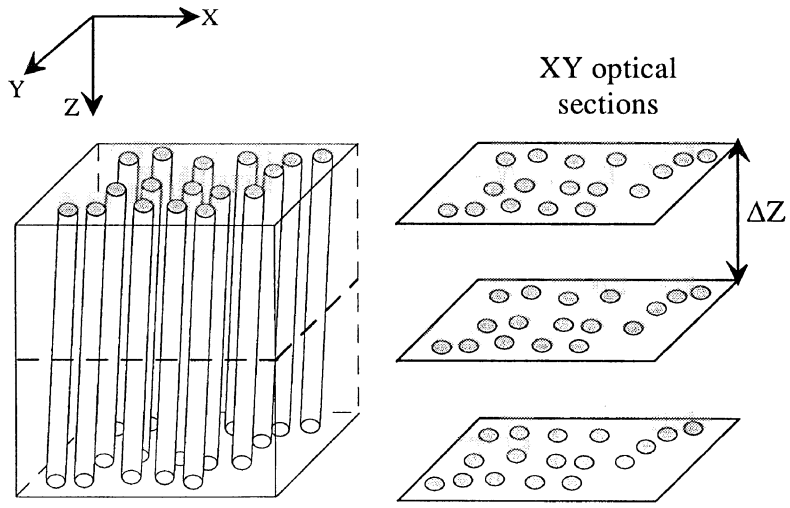

Fig. 1a. One possible technique for 3D reconstruction using the CLSM: xy-image frames taken at different depths, Δz within the sample.

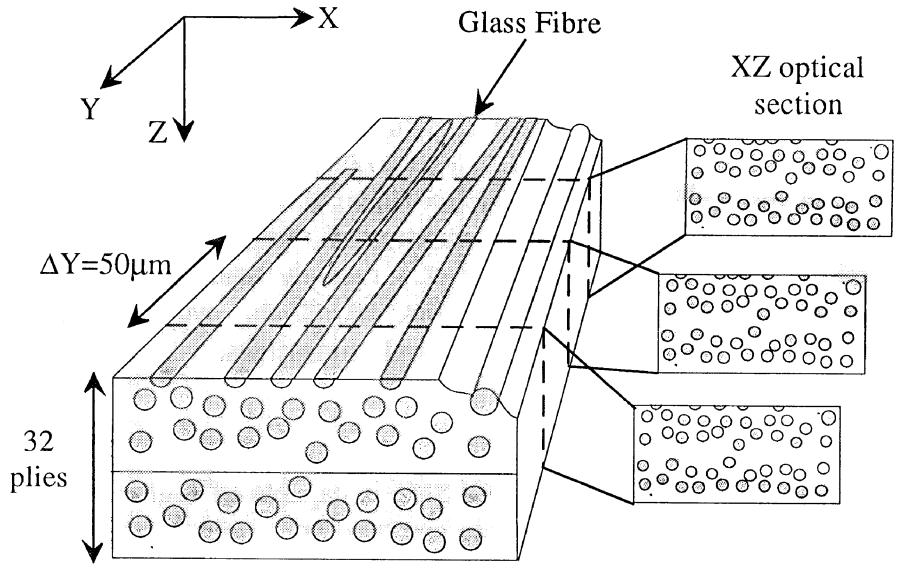

Fig. 1b. Another possible technique for 3D reconstruction using the CLSM: xz-image frames separated by Δy (along the main fibre direction).

system is δx, $\delta y = \pm 0.25$ μm and $\delta z = \pm 0.3$ μm. Fortunately, in glass fibre reinforced epoxies, useful fibre/matrix discrimination can be obtained at depths up to 40 μm below the surface, even at high packing fractions ($v_f = 42\%$).

In order to reconstruct the mesostructure of a composite sample in 3D, we analyse either a set of xy-image frames each separated by a fixed Δz, as shown in Figure 1a, or a set of xz-image frames each separated by a fixed Δy, as shown

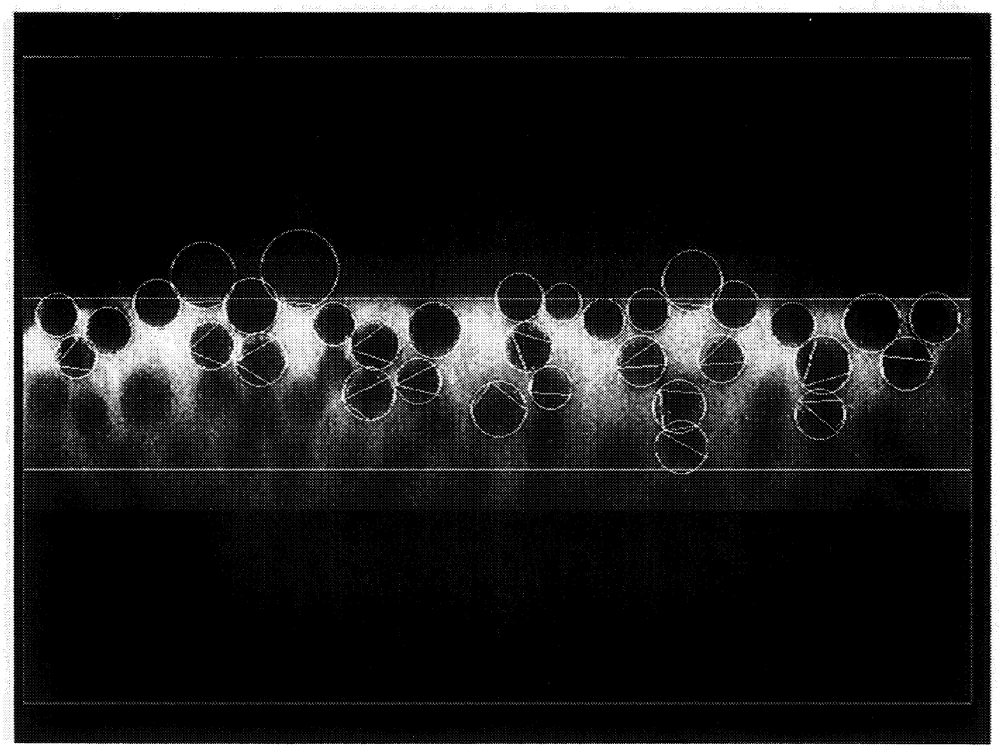

Fig. 2. Typical CLSM xz-image frame showing the dark, circular cross-section, glass fibres and the fluorescing epoxy matrix.

in Figure 1b. Consider a fibre-reinforced composite with the fibres oriented along the y-direction, as in Figure 1b. Peak to peak fibre waviness amplitudes A_w in the z-direction may stay within the measurement window if $A_w \leqslant 40$ μm and, with the system magnification chosen for the pilot study, fibre waviness amplitudes, A_u in the x-direction may stay within the measurement window if $A_u \leqslant 200$ μm. Clearly, with this technique, the fibres which are aligned in the y-direction, may be followed over many mm. As the expected wavelengths were $\lambda \geqslant 0.5$ mm it was decided to choose a separation between xz-image planes, $\Delta y = 50$ μm to ensure adequate spatial sampling of the fibres. A typical xz-image frame is shown in Figure 2.

3. Results and Discussion

An interactive software routine has been written to allow the user to locate the fibre-centre coordinates on each xz-image plane. The user is aided (after the first two xz planes) by a prediction of where the computer expects to find the fibre image on the next xz plane. The operator is able to move the predicted centre to allow for fibre curvature between xz planes. The operator then deals with new fibres entering the xz measurement window and also indicates when the

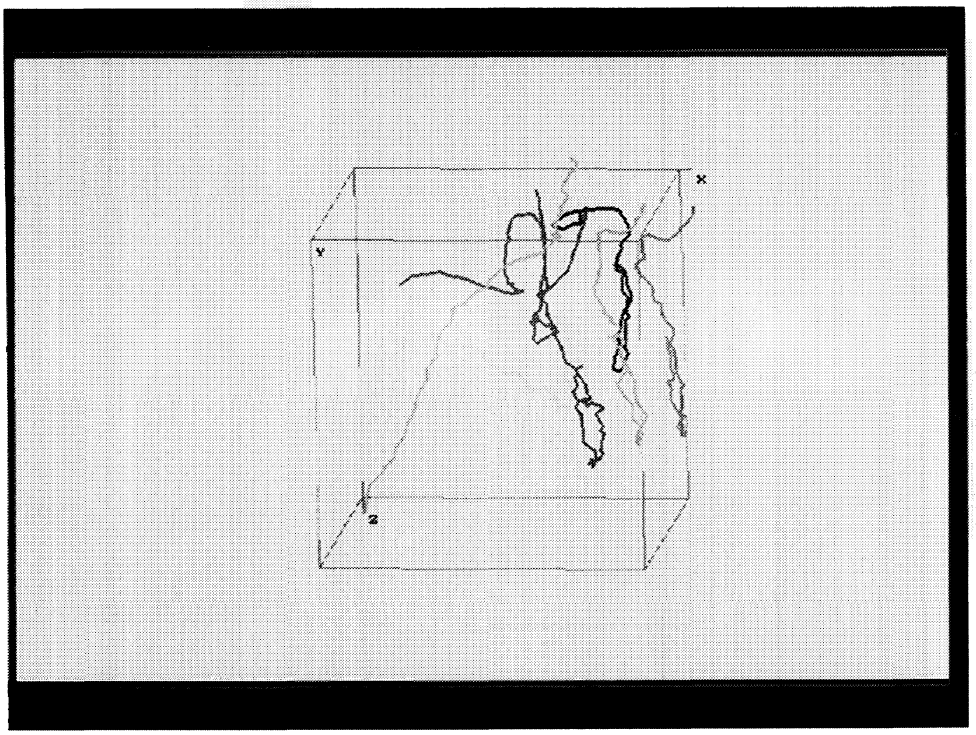

Fig. 3. 3D view of the longest fibres within the dataset. The dimensions of the 3D 'cube' are 40 μm by 5 mm by 30 μm in x, y and z.

fibres have exited the measurement window. In this way, a total of 100 xz-image planes were analysed, covering a total distance of $y = 5$ mm along the sample surface and all of the centre coordinates of glass fibres within a sample volume of 200 μm $\times$ 5mm $\times$ 40 μm were recorded. These data were used to reconstruct the fibres in a 3D 'cube' on the computer screen.

In Figure 3, the seven fibres which were followed for 5 mm with ± 0.3 μm resolution in x, y and z are shown. One of the fibres, shown in greater detail in Figure 4, when viewed end-on indicated that helical motions are possible. In other words, one cannot assume that fibre misalignments in one plane are independent of those misalignments in an orthogonal plane (see for example [4]).

A total of sixteen of the longest fibres in the dataset were used to derive the power spectral densities. Firstly, straight lines were fitted to each fibre and subtracted out so that each fibre has zero mean deviation and zero mean slope. Then the deviations from the mean, $u(y)$ and $w(y)$ were used to compute the power spectral densities, S_u and S_w as indicated by Eqs. (2)–(8). The resulting power spectral densities are shown in Figures 5 and 6. Although of limited statistical significance, this preliminary data does indicate the 'wavelengths' are typically within the region of 0.5 mm $\leqslant \lambda \leqslant$ 4 mm and there is some evidence that the wavelengths in the xy plane were shorter than the wavelength in the zy

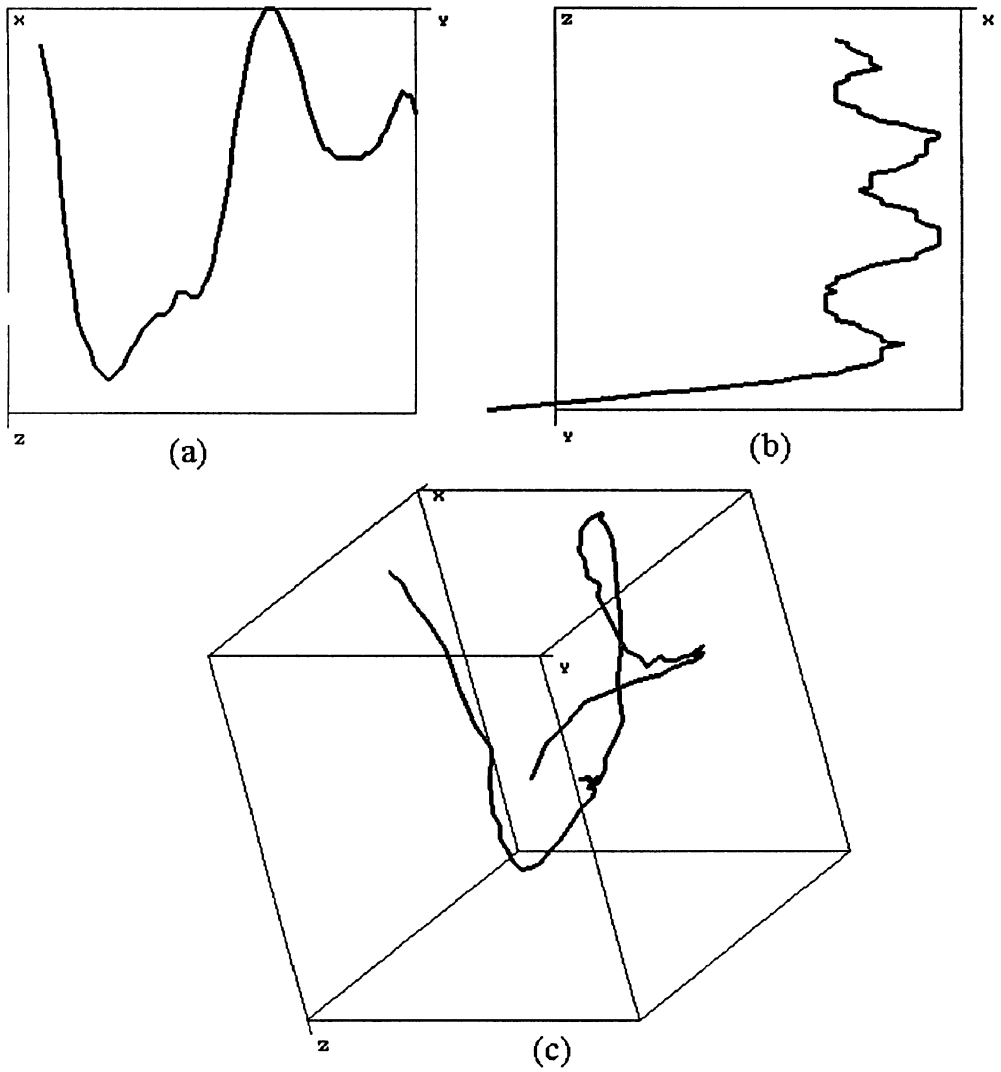

Fig. 4. One of the longest fibres in the dataset, showing correlation between x and z motions over a fibre length of approximately 5 mm: (a) Side elevation view (zy window dimensions 20 μm by 5 mm); (b) Plan view (xy window dimensions 10 μm by 5 mm); (c) 3D 'cube' view (xyz dimensions 10 μm by 5mm by 20 μm).

plane (because of the difference of peak widths in Figures 5 and 6) i.e.

$$0.002\ \mu\text{m}^{-1} < \omega_{S_{u\,\max}} < 0.0045\ \mu\text{m}^{-1}$$
$$\omega_{S_{w\,\max}} < 0.002\ \mu\text{m}^{-1}.$$

Hence, the data suggest that, in the xy plane, wavelengths in the range 3 mm $\geqslant \lambda \geqslant$ 1.4 mm were detected whilst in the zy plane, there was little evidence of wavelengths below 3 mm. This tentative conclusion is consistent with the plan view and side-elevation views of the fibre shown in Figure 4.

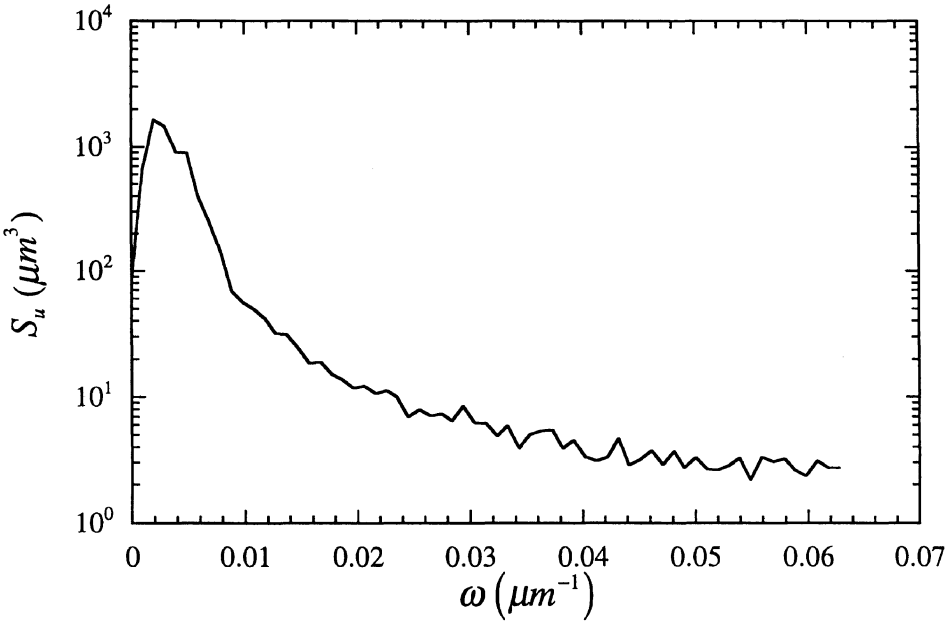

Fig. 5. Power spectral density, S_u μm^3 of fibre deviations in the xy plane.

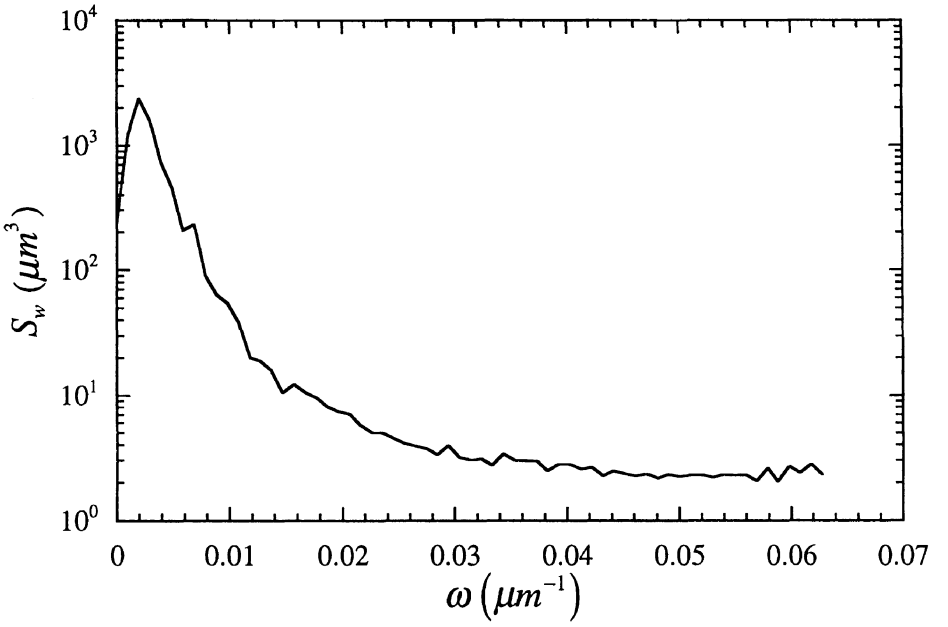

Fig. 6. Power spectral density, S_w μm^3 of fibre deviations in the zy plane.

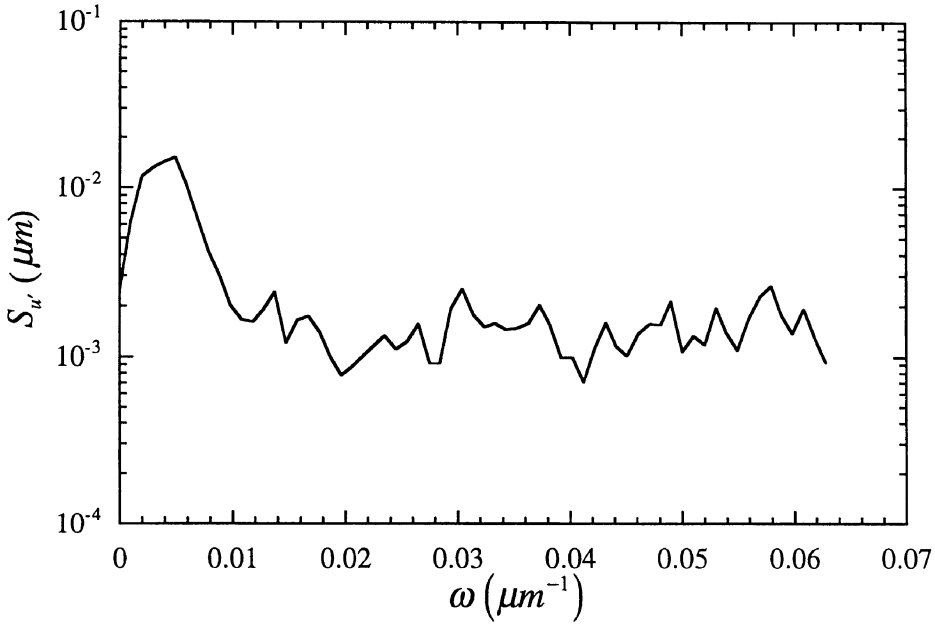

Fig. 7. Spectral density of fibre slopes, $S_{u'}$ μm (fibre misalignment angles in the xy plane).

By automating the fibre-centre detection software and following fibre movement between neighbouring sample volumes and also following fibres for longer distances, better estimates of the power spectral densities should be obtained, resolving the features of the broad spectral distribution peak around frequencies of $\omega = 0.002$ μm^{-1}. Slaughter and Fleck [8] have argued that the random fibre waviness in engineering composites can be characterised by the spectral density of *fibre slope*, $S_{u'}$ and $S_{w'}$ where the fibre slope, m is related to the fibre misalignment angle, Φ by

$$m = \tan \Phi. \tag{9}$$

In the absence of any published data on 3D fibre waviness, they assumed a flat-topped spectral density distribution of fibre slopes, $S_{u'}$ for their Monte Carlo simulations. The spectral density distribution was given a high cut-off frequency, ω_0 which corresponded to a minimum wavelength of 25 fibre diameters. (This cut-off was considered reasonable due to a fibre's finite bending stiffness.) They assumed a mean square value of fibre slope of 4×10^{-4} rads^2.

Using the CLSM technique, the raw fibre-centre coordinates may be used to derive the spectral distribution of fibre slopes in both the xy plane, see Figure 7, and also the zy plane, as shown in Figure 8. The measured mean square values of fibre slopes, $[u']^2 = 3.3 \times 10^{-4}$ rads^2 and $[w']^2 = 2.1 \times 10^{-4}$ rads^2 which implies r.m.s. slope values (i.e. mean misalignment angles) of 1.04° and 0.83°.

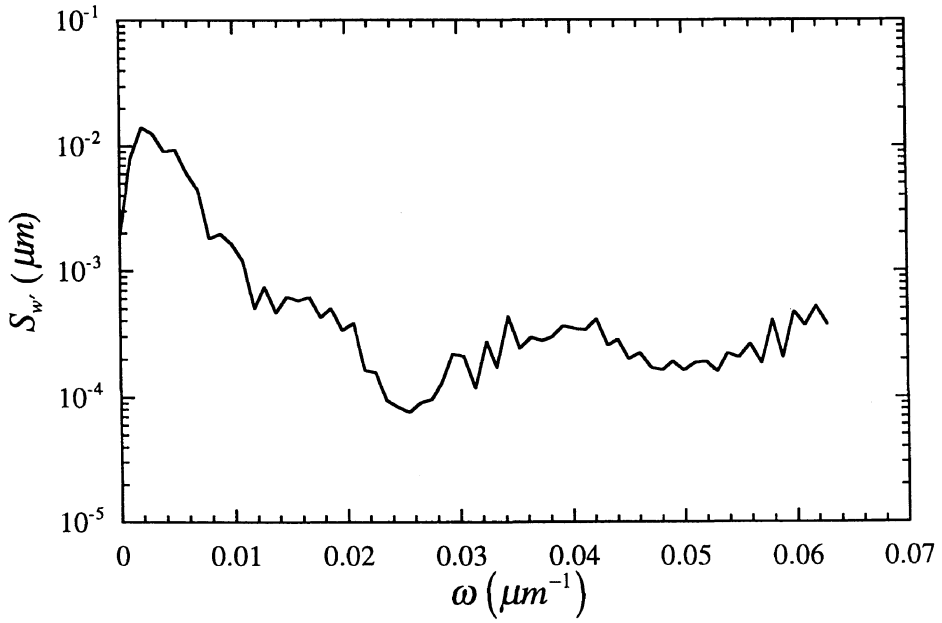

Fig. 8. Spectral density of fibre slopes, $S_{w'}$ μm (fibre misalignment angles in the zy plane).

4. Concluding Remarks

Many composites (e.g. high packing fraction, carbon fibre reinforced) are too opaque for the CLSM to penetrate to sufficient depths below the sample surface. 3D mesostructural studies of carbon fibre reinforced composites may be undertaken with a fully automatic, large area, high spatial resolution, 2D image analyser using pattern matching algorithms to relate fibre images on successively sectioned planes [12]. However, the 2D technique is destructive, whereas the CLSM requires only one single polished section.

At the moment, most commercial CLSM systems allow the user to automate the collection of image data, but more work has to be undertaken to semi-automate the image analysis. Progress is being made in this direction involving strategies for preprocessing of the image data (especially from deep within the composite samples) and automatically pattern matching fibre images between xz-image planes. Once these problems have been overcome, the confocal laser-scanning microscope should become a standard tool for 3D mesostructural studies of glass fibre composites and also thin, transparent films and coatings. The rapid and reliable quantification of low level voidage and the correlation of 3D orientation distributions and in situ fibre length distributions will soon be possible by confocal laser scanning microscopy.

Acknowledgements

ND and GA are both supported on a Brite Euram funded project, BE-8081 and our CLSM algorithms are being improved on this programme together with a fully automated 2D image analyser for the characterisation of opaque composites. Our thanks to Prof. Paul Curtis at DRA (Farnborough) and Dr. Mike Wisnom at the Aerospace Engineering Department, University of Bristol for introducing us to the fibre waviness problem and providing the sample (Fibredux 924/T800 toughened epoxy) investigated in this pilot study. WSS and NAF are grateful for financial support from the Defence Research Agency, Farnborough (programme monitor, Prof. Paul Curtis) and from the ONR (monitor Dr. Y.D.S. Rajapakse, grant No. 0014-91-J1916).

The research would not have been possible without the support and encouragement of Dr. Andrew Dixon at Biorad Microscience Ltd. and the loan of their MRC500 confocal laser scanning microscope system.

References

1. Piggott, M. R., 'Recent Work on Mesostructures and the Mechanics of Fiber Composites', *IUTAM Symposium on Microstructure-Property Interactions in Composite Materials*, Kluwer Academic Publishers, Dordrecht, 1995, 289–300.
2. Budiansky B. and Fleck N. A., 'Compressive Failure of Fibre Composites', *J. Mech. Phys. Solids,* 1993, 183–211.
3. Davis, J. G., 'Compressive Strength of Fibre Reinforced Composite Materials', *Composite Reliability ASTM STP* **580**, 1975, 364–377.
4. Yurgartis, S. W., 'Measurement of Small Angle Fibre Misalignments in Continuous Fibre Composites', *Comp. Sci. Tech.* **30**, 1987, 279–293.
5. Frankle, R. S., 'Detecting and Evaluating Fiber Misalignments in Composite Materials', *Proc. Mesostructures and Mesomechanics in Fiber Composites* (Ed Piggott, Univ. of Toronto), 1994, 56–70.
6. Camponeschi, E. T., 'Lamina Waviness Levels in Thick Composites and Its Effect on Their Compression Strength', *Proc. ICCM8, Honolulu,* 1991, 30-E-1–30-E-13.
7. Wisnom, M. R., 'The Effect of Fibre Waviness on the Relationship between Compressive Strengths of Unidirectional Composites', *J. Composite Materials* **28**(1), 1994, 66–76.
8. Slaughter, W. S. and Fleck, N., 'Microbuckling of Fiber Composites with Random Initial Fiber Waviness', *J. Mech. Phys. Solids* **42**(11), 1994, 1743–1766.
9. Newland, D. E., 'An Introduction to Random Vibrations and Spectral Analysis', Longman Group Publishers, ISBN 0 582 46334 3.
10. Clarke, A. R., Archenhold, G. and Davidson, N., 'A Novel Technique for Determining the 3D Spatial Distribution of Glass Fibres in Polymer Composites', *Comp. Sci. Tech.* **55**, 1995, 75–91.
11. Clarke, A. R., Archenhold, G. and Davidson, N., '3D Confocal Microscopy of Glass Fibre Reinforced Composites', in J. Summerscales (ed.), *Microstructural Characterisation of Fibre Reinforced Composites,* Chapter 2, Woodhead Publishers, publ. date Jan. 1996.
12. Clarke, A. R., Davidson, N. and Archenhold, G., 'Microstructural Characterisation of Aligned Fiber Composites', in D. C. Guell and T. D. Papathanasiou (eds.), *Flow-Induced Alignment in Composite Materials,* Chapter 7, Woodhead Publishers, publ. date May 1996.